PHYSICAL REVIEW B VOLUME 25, NUMBER 4 15 FEBRUARY 1982

Absorption and luminescence of dye-coated silver and gold particles

D.-S. Wang and M. Kerker
Clarkson College of Technology, Potsdam, New York 13676
(Received 8 September 1981)

Formulas are derived for the extinction cross section of small randomly oriented, two-layer spheroids and for the luminescence of small spheres coated with a luminescent layer. Numerical examples are presented showing the dependence of the extinction of dye-coated particles upon the particle size, the optical properties of the core (silver, gold, dielectric), the coating thickness, and the spheroid eccentricity. The interaction of metal and dye extinction bands, the splitting of these bands, and the enhancement of the extinction depend sensitively on these various parameters. The enhancement of the luminescence of dye layers coating metallic spheres is shown to be related to comparable enhancements in the extinction. The present model differs from earlier studies of surface-enhanced Raman scattering (SERS) in that the electric dipoles which simulate the dye molecules are embedded in a medium having the dielectric properties of the dye rather than dangling into the external medium. The present study utilizes air as the external medium. The enhancement effects would be much greater in water.

I. INTRODUCTION

The remarkable enhancement of Raman scattering (SERS) from molecules adsorbed on roughened metal-electrode surfaces,[1] vapor-deposited metal-island films,[2,3] colloidal-metal hydrosols,[4–6] etc., may be accounted for, at least for the most part, by corresponding enhancement of the electromagnetic fields at the molecular sites due to plasma resonances of the metal surface protuberances, metal islands, or colloidal metallic particles, respectively.

Colloids, as noted by Moskovits,[7] form particularly simple model systems because, when sufficiently dilute, they can be treated as an array of incoherently emitting single particles isolated in a dielectric medium. Indeed, an electrodynamic-field theory has been articulated for SERS by colloidal spheres and spheroids in which the active molecules are stimulated by the local field which is comprised of the incident plus the elastically scattered fields. The emitted Raman radiation, in turn, is also scattered by the particle. Very large enhancements occur whenever the incident and reradiated fields excite plasma resonances in the particles. This theory has been applied to colloidal spheres in the limit that the particles are small relative to the wavelength and that the wavelength is not too close to an optical resonance,[8,9] as well as in the general case for homogeneous spheres of any size or optical properties.[10] Spheroids have been treated in the small-particle limit for a single molecule located on the nose of a prolate spheroid illuminated at nose-on incidence[11,12] and also for a monolayer on randomly oriented spheroids.[13]

The origin of SERS in optical resonances has suggested that this phenomena is related to optical absorption by small metal particles,[4] a subject in colloid optics which has a venerable history,[14–16] and it has been proposed that such resonances may have similar effects on metal particles with adsorbed luminescent molecules.[8,10]

Glass *et al.*[17] have measured the absorption, luminescence, and excitation luminescence of layers of dye molecules on silver, gold, and copper-island films. They found strong coupling between the dye and the metal which depends upon the degree of overlap of the dye absorption spectrum with that of the metal islands. In contrast to molecules close to smooth, continuous metal surfaces, for which the luminescence is heavily quenched, enhanced luminescence was observed for dyes adsorbed on small metal islands. By interposing a 30-Å-thick layer of polymethyl methacrylate between the silver and the dye, these authors have shown that the effect is primarily electromagnetic. Direct contact with silver is not necessary, as is also observed with SERS.[18] More recently Garoff *et al.*[19] have verified the main features of the optical-absorption resonances of such dye-coated silver-island films.

Craighead and Glass[20] have attempted to account for the measured absorption spectra of the dye-coated silver-island films[17] with the effective-medium theory of Maxwell-Garnett.[16] They modeled the scattering particles by Guttler's expression for the electric-dipole limit[21] of the elastic scattering by concentric spheres of arbitrary size and optical constants.[21,22] Garoff *et al.*[19] calculated the absorption spectra for particles comprised of a silver spheroid coated with a layer of dye whose outer boundary is confocal with the silver core. By assuming that the particle is small compared to the wavelength, the electric fields can be obtained in the dipole limit by solving Laplace's equation. Solutions for the concentric sphere as well as the two-layer confocal spheroid can also be obtained by appropriate reduction of the more general ellipsoidal case.[23,24] Eagen[25] extended the results of Garoff *et al.* using an approach somewhat different from the Maxwell-Garnett treatment. The local field in the layer of spheroids was obtained by assuming a hexagonal lattice of particles, followed by a self-consistent calculation of the static dipole fields from all the dipoles of the lattice. Interactions with the substrate were treated by including in the lattice sums a contribution for each spheroid from an image dipole in the substrate. This leads to an equivalent thin film with effective dielectric functions for which the optical properties can be computed by employing the Fresnel relations. Each of these approaches[20,25] was able to simulate the qualitative features of the experimentally observed coupling between the dyes.

In this paper, we limit the analysis and computations of the dye-metal interactions to randomly oriented isolated particles as our experimental work will proceed in that direction, viz., absorption and luminescence of dilute colloidal dispersions comprised of dye-coated metal particles. Yet the results may be of more general interest since the physics is exposed more directly, and in any case, single-particle optics must be utilized in treating a system of interacting particles.

Section II provides the formalism for calculation of the extinction cross section of a randomly oriented two-layer spheroid. Next we treat luminescence. The electrodynamic model for inelastically scattering (including luminescent) molecules embedded within small particles had been formulated earlier for spheres,[26–29] concentric spheres,[30] circular cylinders,[31] and spheroids,[32] and numerical results were presented for each case except for the concentric spheres. The concentric sphere model is applicable to a luminescent layer on a metal core which is under investigation here. This differs from the earlier electrodynamic treatment[10] of SERS in that the active molecules are now treated as electric dipoles embedded within a spherical shell having the bulk dielectric properties of the coating material, rather than as a monolayer dangling out in the medium external to the particle. Because the full series expansion for concentric spheres requires considerable programming and computation time,[30] we present in Sec. III, a more limited analysis which is valid only for particles which are small compared to the wavelength.

Numerical results are presented in Sec. IV for silver, gold, and dielectric cores coated with a layer of dye. The dielectric constant data of Johnson and Christy[33] were used for silver and gold; a Lorentzian form with the same constants used by Craighead, and Glass[20] was taken to simulate a dye such as Rhodamine B. In Sec. IV A extinction cross sections are given for concentric spheres using the general formalism of Aden and Kerker.[22] This is not limited to the dipole limit (particles small compared to wavelength) used by earlier workers.[20] The extinction cross sections for randomly oriented confocal spheroids are given in Sec. IV B. Finally, the enhancement of luminescence by dye-coated silver spheres in the small-particle limit, is given in Sec. IV C.

II. EXTINCTION CROSS SECTION OF A SMALL RANDOMLY ORIENTED, TWO-LAYER SPHEROID

Consider (see Fig. 1) a two-layer confocal spheroid of semimajor axis a and semiminor axis b. The corresponding axes of the core, l and n, are

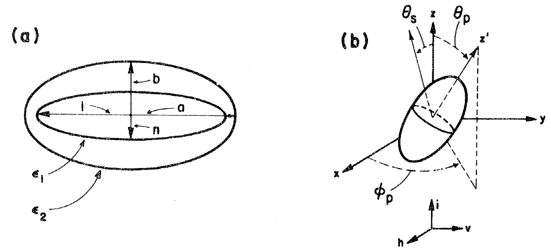

FIG. 1. (a) Spheroidal particle with semiaxes a, b, and n, l, and dielectric constants ϵ_1 and ϵ_2. (b) Scattering geometry. Orientation of spheroid determined by θ_p, ϕ_p; scattering angle θ_s; incident direction is i; polarization directions parallel and perpendicular to the $x-z$ plane are h and v.

$$l=a[1-d^2]^{1/2}\,,$$

$$n=a[(b/a)^2-d^2]^{1/2}\equiv a[\gamma^2-d^2]^{1/2}\,,$$

where d can be any value between 0 and 1, and $\gamma=b/a$. The dielectric constants of the core and coating relative to the surrounding medium are ϵ_1 and ϵ_2, respectively.

For dimensions small compared to the incident wavelength ($a,b<<\lambda_0$), the scattering can be approximated by the radiation of the dipole located at the center of the spheroid with dipole moment,

$$\vec{p}'=\alpha'_{||}E'_{0z}\hat{z}'+\alpha'_{\perp}(E'_{0x}\hat{x}'+E'_{0y}\hat{y}')\,, \tag{1}$$

where $\hat{x}'$, $\hat{y}'$, and $\hat{z}'$ are the unit vectors along the axes of the prime coordinates which are fixed on the spheroid with the z' axis along the axis of symmetry. $E'_{0x'}$, $E'_{0y'}$, and $E'_{0z'}$ are the components of the incident electric field. $\alpha'_{||}$ and $\alpha'_{\perp}$ can be shown to be given by[24]

$$\alpha'_{\perp,||}=-\frac{2}{3}\,\frac{R_{\perp,||}a^3-\epsilon_2(S_{\perp,||}a^3}{\epsilon_2(S_{\perp,||}a^3)(B_{\perp,||}a^3)-(R_{\perp,||}a^3)(B_{\perp,||}a^3)+2(R_{\perp,||}a^3)/\gamma^2}\,a^3 \tag{2}$$

where

$$R_{\perp,||}a^3=B_{\perp,||}a^3-A_{\perp,||}a^3-\frac{\epsilon_2}{\epsilon_1-\epsilon_2}\,\frac{2}{(1-d^2)^{1/2}(\gamma^2-d^2)}\,, \tag{3}$$

$$S_{\perp,||}a^3=R_{\perp,||}a^3-\frac{2}{\gamma^2}\,,$$

$B_{\perp,||}$ and $A_{\perp,||}$ are

$$B_{||}a^3=\frac{2}{1-\gamma^2}\left[\frac{1}{2(1-\gamma^2)^{1/2}}\ln\frac{1+(1-\gamma^2)^{1/2}}{1-(1-\gamma^2)^{1/2}}-1\right],$$

$$A_{||}a^3=\frac{2}{(1-\gamma^2)^{3/2}}\left[\frac{1}{2}\ln\frac{1+\left[\dfrac{1-\gamma^2}{1-d^2}\right]^{1/2}}{1-\left[\dfrac{1-\gamma^2}{1-d^2}\right]^{1/2}}-\left[\frac{1-\gamma^2}{1-d^2}\right]^{1/2}\right], \tag{4}$$

$$B_{\perp}a^3=\frac{1}{\gamma^2}-\frac{1}{(1-\gamma^2)^{3/2}}\left[\frac{1}{2}\ln\frac{1+(1-\gamma^2)^{1/2}}{1-(1-\gamma^2)^{1/2}}-(1-\gamma^2)^{1/2}\right],$$

$$A_{\perp}a^3=\frac{1}{(\gamma^2-d^2)(1-d^2)^{1/2}}-\frac{1}{(1-\gamma^2)^{3/2}}\left[\frac{1}{2}\ln\frac{1+\left[\dfrac{1-\gamma^2}{1-d^2}\right]^{1/2}}{1-\left[\dfrac{1-\gamma^2}{1-d^2}\right]^{1/2}}-\left[\frac{1-\gamma^2}{1-d^2}\right]^{1/2}\right],$$

for prolate spheroids, and

$$B_{||}a^3=\frac{2}{\gamma^2-1}-\frac{2}{(\gamma^2-1)^{3/2}}\sin^{-1}\frac{(\gamma^2-1)^{1/2}}{\gamma}\,,$$

$$A_{||}a^3=\frac{2}{(\gamma^2-1)(1-d^2)^{1/2}}-\frac{2}{(\gamma^2-1)^{3/2}}\sin^{-1}\frac{(\gamma^2-1)^{1/2}}{(\gamma^2-d^2)^{1/2}}\,, \tag{5}$$

$$B_{\perp}a^3=\frac{1}{\gamma^2}-\frac{1}{\gamma^2-1}+\frac{1}{(\gamma^2-1)^{3/2}}\sin^{-1}\frac{(\gamma^2-1)^{1/2}}{\gamma}\,,$$

$$A_{\perp}a^3=\frac{1}{(\gamma^2-d^2)(1-d^2)^{1/2}}-\frac{1}{(\gamma^2-1)(1-d^2)^{1/2}}+\frac{1}{(\gamma^2-1)^{3/2}}\sin^{-1}\frac{(\gamma^2-1)^{1/2}}{(\gamma^2-d^2)^{1/2}}\,,$$

for oblate spheroids.

Therefore, the scattered electric field (sc) in the radiation zone due to the presence of the spheroid is given by

$$\vec{E}'_{\mathrm{sc}}=\frac{e^{ik_0 r'}}{r'}k_0^2(\hat{r}'\times\vec{p}')\times\hat{r}' \ , \tag{6}$$

where k_0 is equal to $2\pi/\lambda_0$, and $\hat{r}'$ is a unit vector in the $x'y'z'$ coordinates along the direction of observation. The far-field amplitude $\vec{F}'$ in the $x'y'z'$ coordinates is defined by

$$\vec{F}'(\hat{r}')=k_0^2(\hat{r}'\times\vec{p}')\times\hat{r}' \ ,$$

or

$$\vec{F}'(\hat{r}')=k_0^2[\vec{p}'-\hat{r}'(\hat{r}'\cdot\vec{p})] \ . \tag{7}$$

Because of the random orientation of the spheroid, a second coordinate system, namely xyz, is needed. The incident wave propagates along the z axis with the electric field either along the x axis, which is referred to as the horizontal polarization, or along the y axis, which is referred to as the vertical polarization. The orientation of the spheroid can then be defined by the direction of the z' axis relative to the xyz coordinates in terms of the angles θ_p and ϕ_p. Any vector given in the xyz coordinates can be transformed to the $x'y'z'$ coordinates using the transformation matrix $[T]$:

$$[T]=\begin{bmatrix}\cos\theta_p\cos\phi_p & \cos\theta_p\sin\phi_p & -\sin\theta_p\\ -\sin\phi_p & \cos\phi_p & 0\\ \sin\theta_p\cos\phi_p & \sin\theta_p\sin\phi_p & \cos\theta_p\end{bmatrix} \ . \tag{8}$$

The inverse transformation can be carried out by using $[T]^{\dagger}$, the transpose of $[T]$.

Therefore, for a given orientation of the spheroid, the far-field amplitude $\vec{F}$ observed in the xyz coordinates is given by

$$\vec{F}(\hat{r})=[T]^{\dagger}\vec{F}'(\hat{r}') \ , \tag{9}$$

where $\hat{r}=[T]^{\dagger}\hat{r}'$. Substituting Eq. (7) into Eq. (9) and using the transformation matrix $[T]$ gives

$$\vec{F}(\hat{r})=k_0^2(\underline{1}-\hat{r}\hat{r})\cdot([T]^{\dagger}\vec{p}') \ . \tag{10}$$

We may rewrite Eq. (1) to become

$$\vec{p}'=\alpha'\vec{E}_0{}'=\alpha'[T]\vec{E}_0 \ , \tag{11}$$

where $\vec{E}'_0$ and $\vec{E}_0$ represent the incident electric field in the $x'y'z'$ coordinates and the xyz coordinates, respectively, and α' is a second-rank tensor given by

$$\alpha'=\begin{bmatrix}\alpha'_{\parallel} & 0 & 0\\ 0 & \alpha'_{\parallel} & 0\\ 0 & 0 & \alpha'_{\perp}\end{bmatrix} \ . \tag{12}$$

Substituting Eq. (11) into Eq. (10) gives

$$\vec{F}(\hat{r})=k_0^2(\underline{1}-\hat{r}\hat{r})\cdot(\alpha\vec{E}_0) \ , \tag{13}$$

where α is also a second-rank tensor given by

$$\alpha=(T)^{\dagger}\alpha'(T) \ . \tag{14}$$

According to the optical theorem, the extinction cross section C_{ext} is given by

$$C_{\mathrm{ext}}=\frac{4\pi}{k_0}\mathrm{Im}[\hat{\epsilon}_0^{*}\cdot\vec{F}(\hat{r}=\hat{z})] \tag{15}$$

where $\hat{\epsilon}_0^{*}$ is parallel to $\vec{E}_0$, and we have let $|\vec{E}_0|=1$. It can be seen from Eqs. (13) and (14) that the calculation of C_{ext} of a randomly oriented spheroid in the xyz coordinates involves the evaluation of $\bar{\alpha}$ which is defined as the average of α over orientation. For $\vec{E}_0$ along either the x or y axis, $\hat{\epsilon}_0^{*}\cdot\vec{F}(\hat{r}=\hat{z})$ of a randomly oriented spheroid, can be shown and given by

$$\hat{\epsilon}_0^{*}\cdot\vec{F}(\hat{r}=\hat{z})=\frac{k_0^2}{3}(2\alpha'_{\parallel}+\alpha'_{\perp}) \ . \tag{16}$$

Substituting Eq. (16) into Eq. (15), we obtain the extinction cross section $\bar{C}_{\mathrm{ext}}$ of a randomly oriented spheroid given by

$$\bar{C}_{\mathrm{ext}}=\frac{4\pi}{3}k_0\mathrm{Im}(2\alpha'_{\parallel}+\alpha'_{\perp}) \ . \tag{17}$$

III. ENHANCEMENT OF LUMINESCENCE BY A SMALL SPHERE COATED WITH A LUMINESCENT LAYER

We continue with the standard model in which an active molecule, treated as an electric dipole, is stimulated by the local field at the incident frequency and subsequently reradiates at the shifted frequency, also as an electric dipole. Radiation from a macroscopic region, in this case from a concentric shell surrounding a spherical core, is obtained by addition of the electric fields or Poynting vectors of a sufficiently dense array of dipoles, depending upon whether the emission is coherent or incoherent, respectively. Enhancement is obtained by comparison with emission by a randomly oriented molecule in the external medium having the same polarizabilities for absorption and emission as the embedded molecule. Should any perturbation of the polarizabilities of the embedded molecules from those of the free molecules be known, that can be included in the formalism. However, in this model we consider only the effects of the influence of the particle upon the electromagnetic fields. We omit consideration of the nonradiative decay channels (i.e., formation of *e-h* pairs, plasmons, etc.) of the molecules' interactions with the metallic substrate. Since these can be large for short molecule-metal distances and perhaps frequency dependent as well, this calculation better approximates the case of dye molecules spaced away from the metal. Accordingly it provides an upper limit for fluorescence enhancement.

As noted earlier, here we will treat the limiting case of a particle which is small compared to the wavelength in order to avoid the lengthy programming and computations required for the general case which had been presented earlier.[30] The small-particle limit requires solution only of the electrostatic problem.

We proceed firstly with an evaluation of the electric field in the coating of a two-layer sphere. Consider a two-layer sphere with inner and outer radii a and c, respectively. The dielectric constants relative to the surrounding medium are ϵ_1 and ϵ_2 for the core and coating, respectively. The magnetic permeability throughout is considered to be that in vacuum. For an electromagnetic wave incident along the x axis with the electric field $\vec{E}_0$ parallel to the z axis, the potentials in the three regions can be represented by

$$\begin{aligned}\phi_1(\omega_0)&=\sum_{l=0}^{\infty}A_l r^l P_l(\cos\theta)\ ,\\ \phi_2(\omega_0)&=\sum_{l=0}^{\infty}(B_l r^l+C_l r^{-(l+1)})P_l(\cos\theta)\ ,\\ \phi_3(\omega_0)&=\sum_{l=0}^{\infty}D_l r^{-(l+1)}P_l(\cos\theta)-E_0 r\cos\theta\ .\end{aligned}\qquad(18)$$

Applying the boundary conditions that the tangential component of $\vec{E}$ and the normal component of $\vec{D}$ are continuous at both boundary surfaces ($r=a,c$), the nonzero coefficients are given by

$$\begin{aligned}A_1&=\frac{9\epsilon_2}{(\epsilon_2+2)(\epsilon_1+2\epsilon_2)+2(a/c)^3(\epsilon_2-1)(\epsilon_1-\epsilon_2)}E_0\ ,\\ B_1&=-\frac{3(\epsilon_1+2\epsilon_2)}{(\epsilon_2+2)(\epsilon_1+2\epsilon_2)+2(a/c)^3(\epsilon_2-1)(\epsilon_1-\epsilon_2)}E_0\ ,\\ C_1&=\frac{3(\epsilon_1-\epsilon_2)}{(\epsilon_2+2)(\epsilon_1+2\epsilon_2)+2(a/c)^3(\epsilon_2-1)(\epsilon_1-\epsilon_2)}(a^3E_0)\ ,\\ D_1&=\frac{(\epsilon_1+2\epsilon_2)(\epsilon_2-1)+(a/c)^3(\epsilon_1-\epsilon_2)(2\epsilon_2+1)}{(\epsilon_2+2)(\epsilon_1+2\epsilon_2)+2(a/c)^3(\epsilon_2-1)(\epsilon_1-\epsilon_2)}(c^3E_0)\ .\end{aligned}\qquad(19)$$

Substituting Eq. (19) into Eq. (18) gives

$$\begin{aligned}\phi_1(\omega_0)&=A_1 r\cos\theta\ ,\\ \phi_2(\omega_0)&=(B_1 r+C_1 r^{-2})\cos\theta\ ,\\ \phi_3(\omega_0)&=(D_1 r^{-2}-E_0 r)\cos\theta\ .\end{aligned}\tag{20}$$

The electric fields are

$$\begin{aligned}\vec{E}_1&=A_1(-\cos\theta\hat{r}+\sin\theta\hat{\theta})\ ,\\ \vec{E}_2&=(-B_1+2C_1 r^{-3})\cos\theta\hat{r}\\ &\quad+(B_1+C_1 r^{-3})\sin\theta\hat{\theta}\ ,\\ \vec{E}_3&=(2D_1 r^{-3}+E_0)\cos\theta\hat{r}\\ &\quad+(D_1 r^{-3}-E_0)\sin\theta\hat{\theta}\ .\end{aligned}\tag{21}$$

It can be seen that $\vec{E}_1$ is a constant field parallel to the z axis, $\vec{E}_2$ is the sum of a constant field in the z direction and a field proportional to r^{-3}, and $\vec{E}_3$ is the incident field $\vec{E}_0$ plus the scattered field which can be considered as the field due to an electric dipole located at the center of the sphere with dipole moment D_1.

Next we consider a molecule located at (r',θ',ϕ') in the coating, and assume that it is oriented radially with polarizability $\hat{r}'\hat{r}'$. Therefore, the dipole induced at the location of the molecule has a dipole moment given by

$$\vec{p}_m=(2C_1 r'^{-3}-B_1)\cos\theta'\hat{r}'\ ,\tag{22}$$

with corresponding potential given by

$$\begin{aligned}\phi_m&=\frac{\vec{p}_m\cdot\vec{R}}{R^3},\quad \vec{R}=|\vec{r}-\vec{r}'|\\ \phi_m&=-\vec{p}_m\cdot\left[\vec{\nabla}\frac{1}{R}\right]\ .\end{aligned}\tag{23}$$

Since $1/R$ can be expanded as

$$\frac{1}{R}=4\pi\sum_{l=0}^{\infty}\sum_{m=-l}^{l}\frac{1}{2l+1}\frac{r<l}{r>l+1}Y_m^*(\theta',\phi')Y_{lm}(\theta,\phi)\ ,\tag{24}$$

the potential due to the dipole $\vec{p}_m$ in the coating can be represented by

$$\phi_m=(-4\pi p_m)\times\begin{cases}\displaystyle\sum_{l=0}^{\infty}\sum_{m=-l}^{l}\frac{l}{2l+1}\frac{r'^{l-1}}{r^{l+1}}Y_{lm}^*(\theta',\phi')Y_{lm}(\theta,\phi), & r'<r\\ \displaystyle\sum_{l=0}^{\infty}\sum_{m=-l}^{l}\frac{-(l+1)}{2l+1}\frac{r^l}{r'^{l+2}}Y_{lm}^*(\theta',\phi')Y_{lm}(\theta,\phi), & r'>r\end{cases}\tag{25}$$

where

$$p_m=(2C_1 r'^{-3}-B_1)\cos\theta'$$

is the magnitude of $\vec{p}_m$, (r,θ,ϕ) are the coordinates at which the potential is evaluated, and $Y_{lm}(\theta,\phi)$ is the spherical harmonic given by

$$Y_{lm}(\theta,\phi)=\left[\frac{(2l+1)(l+m)!}{4\pi(l+m)!}\right]^{1/2}p_l^m(\cos\theta)e^{im\phi}\ .$$

Because of the presence of the oscillating dipole $\vec{p}_m$ at the shifted frequency ω, there also exists a corresponding potential in each region which can be expanded as follows:

$$\begin{aligned}\phi_1(\omega)&=\sum_{l=0}^{\infty}\sum_{m=-l}^{l}(\lambda_{lm}r^l)Y_{lm}(\theta,\phi)\ ,\\ \phi_2(\omega)&=\phi_m+\sum_{l=0}^{\infty}\sum_{m=-l}^{l}(B_{lm}r^l+\delta_{lm}r^{-(l+1)})Y_{lm}(\theta,\phi)\ ,\\ \phi_3(\omega)&=\sum_{l=0}^{\infty}\sum_{m=-l}^{l}\alpha_{lm}r^{-(l+1)}Y_{lm}(\theta,\phi)\ ,\end{aligned}\tag{26}$$

where $\phi_1(\omega)$, $\phi_2(\omega)$, and $\phi_3(\omega)$ correspond to the inelastic part of the potential in the core, in the coating, and outside the sphere, respectively.

We apply the same boundary conditions at each boundary as in solving the elastic part of the problem in order to obtain the coefficients α_{lm}, β_{lm}, δ_{lm}, and λ_{lm} using the known potential ϕ_m given in Eq. (25). Since we are interested here in calculating the luminescent scattered field, only the solution of α_{lm} is presented here. It is given by

$$\alpha_{lm}=(-4\pi p_m)\frac{l\epsilon_2'\{[(l+1)\epsilon_2'+l\epsilon_1']+(l+1)(a/r')^{2l+1}(\epsilon_l'-\epsilon_2')\}}{[l\epsilon_2'+(l+1)][l\epsilon_1'+(l+1)\epsilon_2']+l(l+1)(a/c)^{2l+1}(\epsilon_2'-1)(\epsilon_1'-\epsilon_2')}[r'^{l-1}Y_{lm}^*(\theta',\phi')]\ , \tag{27}$$

where ϵ_1' and ϵ_2' are the dielectric constants at the shifted frequency ω relative to the surrounding medium. It can be seen from Eq. (27) that for $l=0$, $\alpha_{0m}=0$. For $l\geq 1$, since $\alpha_{lm}\propto r'^{l-1}$, we may neglect $l>1$ terms in the expansion of $\phi_3(\omega)$ in Eq. (26) for $r'<<\lambda_0$. Therefore, $\phi_3(\omega)$ is given by

$$\phi_3(\omega)=\sum_{m=-1}^{1}\alpha_1 r^{-2}Y_{lm}^*(\theta',\phi')Y_{lm}(\theta,\phi)\ , \tag{28}$$

where

$$\alpha_1=(-4\pi p_m)\frac{\epsilon_2'[(\epsilon_1'+2\epsilon_2')+2(a/r')^3(\epsilon_1'-\epsilon_2')]}{[(\epsilon_2'+2)(\epsilon_1'+2\epsilon_2')+2(a/c)^3(\epsilon_1'-\epsilon_2')(\epsilon_2'-1)]}\ .$$

Note that α_{lm} is independent of m. Summing over m in Eq. (28) gives

$$\phi_3(\omega)=\frac{3}{4\pi}\alpha_1 r^{-2}\cos\mathcal{X}\ , \tag{29}$$

where $\mathcal{X}$ is the angle between $\hat{r}'$ and $\hat{r}$, and is given by

$$\cos\mathcal{X}=\cos\theta'\cos\theta+\sin\theta\sin\theta'\cos(\phi-\phi')\ .$$

According to Eq. (29), it can be shown that the luminescent scattered field $\vec{E}_s(\omega)$ in the radiation zone is the field due to a dipole located at the center of the sphere with dipole moment $\vec{p}_r$,

$$\vec{p}_r=-9\alpha_r(\omega_0)\alpha_r(\omega)E_0\cos\theta'\hat{r}'\ , \tag{30}$$

where $\alpha_r(\omega_0)$ and $\alpha_r(\omega)$ are given by

$$\begin{aligned}\alpha_r(\omega_0)&=\frac{(\epsilon_1+2\epsilon_2)+2(a/r')^3(\epsilon_1-\epsilon_2)}{(\epsilon_2+2)(\epsilon_1+2\epsilon_2)+2(a/c)^3(\epsilon_2-1)(\epsilon_1-\epsilon_2)}\ ,\\ \alpha_r(\omega)&=\frac{\epsilon_2'[(\epsilon_1'+2\epsilon_2')+2(a/r')^3(\epsilon_1'-\epsilon_2')]}{(\epsilon_2'+2)(\epsilon_1'+2\epsilon_2')+2(a/c)^3(\epsilon_2'-1)(\epsilon_1'-\epsilon_2')}\ .\end{aligned} \tag{31}$$

Therefore, for the incident wave propagating along the x axis with the electric field polarized in the z axis, the luminescent scattered field in the radiation zone is given by

$$\vec{E}_s(\omega)=\frac{e^{ikr}}{r}(k^2)[\vec{p}_r-\hat{r}(\hat{r}\cdot\vec{p}_r)]\ , \tag{32}$$

where $k=\omega/c$. The luminescent intensity at a given scattering angle (θ_s,ϕ_s) is directly proportional to the square of the far-field amplitude given by

$$|\vec{F}(\theta_s,\phi_s)|^2=k^4|\vec{p}_r-\hat{r}(\hat{r}\cdot\vec{p}_r)|^2\ . \tag{33}$$

$|\vec{F}(\theta_s,\phi_s)|^2$, given in Eq. (33) is due to a molecule located at (r',θ',ϕ') and oriented radially. For a layer of incoherently emitting molecules we have to sum over $|\vec{\mathrm{F}}(\theta_s,\phi_s)|^2$ due to each molecule.

It can be shown that $|\vec{\mathrm{F}}(\theta_s,\phi_s)|^2$ per molecule for a layer located at r' is that given in Eq. (33) averaged over θ' and ϕ'. $|\vec{\mathrm{F}}(\theta_s,\phi_s)|^2$ can be separated into four polarized components:

$$\begin{aligned}
|F_{H_h}|^2_{\text{layer}} &= k^4|9\alpha_r(\omega_0)\alpha_r(\omega)|^2 \\
&\quad\times[\tfrac{1}{15}(1+2\sin^2\theta_s)]\ , \\
|F_{H_v}|^2_{\text{layer}} &= k^4|9\alpha_r(\omega_0)\alpha_r(\omega)|^2\tfrac{1}{15}\ , \\
|F_{V_v}|^2_{\text{layer}} &= k^4|9\alpha_r(\omega_0)\alpha_r(\omega)|^2\tfrac{1}{5}\ , \\
|F_{V_h}|^2_{\text{layer}} &= k^4|9\alpha_r(\omega_0)\alpha_r(\omega)|^2\tfrac{1}{15}\ ,
\end{aligned} \tag{34}$$

where we have let $E_0=1$. H and V denote that the electric vector of the inelastically scattered field vibrates parallel and perpendicular, respectively, to the scattering plane, which in turn is formed by the incident and scattered directions. The subscripts h and v denote the corresponding polarization of the incident wave.

The enhancement can be determined following the same procedure used earlier for SERS[8,10] by comparing Eq. (34) with $|\vec{\mathrm{F}}(\theta_s,\phi_s)|^2$ for a randomly oriented free molecule given by

$$\begin{aligned}
|F_{H_h}|^2 &= k^2[\tfrac{1}{15}(1+2\sin^2\theta_s)]\ , \\
|F_{H_v}|^2 &= k^4\tfrac{1}{15}\ , \\
|F_{V_v}|^2 &= k^4\tfrac{1}{5}\ , \\
|F_{V_h}|^2 &= k^4\tfrac{1}{15}\ ,
\end{aligned} \tag{35}$$

where the use of $\sin^2\theta_s$, instead of $\cos^2\theta_s$ as in our previous paper is due to the difference in the coordinate system chosen with respect to the incident beam. The incident wave in the previous paper is along the z axis while in this paper it is along the x axis. Therefore a rotation of 90° in the scattering plane (xz plane) is necessary.

It can be seen by comparing Eqs. (34) and (35) that the enhancement is same for any of the four polarization components and is equal to

$$G_{\text{layer}}=|9\alpha_r(\omega_0)\alpha(\omega)|^2\ . \tag{36}$$

The luminescent scattering due to all the molecules in the coating is the incoherent sum of the scattering due to each molecule. The averaged enhancement per molecule is the average of $|\alpha_r(\omega_0)\alpha_r(\omega)|^2$ over r',

$$G_{\text{shell}}=\frac{3}{(c^3-a^3)}\times\int_a^c|9\alpha_r(\omega_0)\alpha_r(\omega)|^2r'^2dr'\ . \tag{37}$$

We have up to now considered the case in which the polarizability of the molecules is $\hat{r}'\hat{r}'$ so that $\vec{\mathrm{p}}_m$ is parallel to $\hat{r}'$. Let us now consider the other possibility that the polarizability of the molecule is $\hat{\eta}\hat{\eta}$ for $\hat{\eta}$ being perpendicular to $\hat{r}'$ and making angle ζ with $\hat{\theta}'$, i.e.,

$$\hat{\eta}=\cos\zeta\,\hat{\theta}'+\sin\zeta\,\hat{\phi}'\ .$$

The procedure in evaluating the fluorescent scattered field $\vec{\mathrm{E}}_s(\omega)$ is very similar to the previous case where $\vec{\mathrm{p}}_m\,||\,\hat{r}'$. However, the expansion of ϕ_m is now given by

$$\phi_m=4\pi p_m\begin{cases}\displaystyle\sum_{l=0}^{\infty}\sum_{m=-l}^{l}\frac{1}{2l+1}\frac{r'^{l-1}}{r'^{l+1}}W_{lm}Y_{lm}(\theta,\phi), & r'<r\\[2ex] \displaystyle\sum_{l=0}^{\infty}\sum_{m=-l}^{l}\frac{1}{2l+1}\frac{r^l}{r^{l+2}}W_{lm}Y_{lm}(\theta,\phi), & r'>r\end{cases} \tag{38}$$

where

$$W_{lm}=\left[\cos\zeta\frac{\partial}{\partial\theta'}+\frac{\sin\zeta}{\sin\theta'}\frac{\partial}{\partial\phi'}\right]Y^*_{lm}(\theta',\phi')\ ,$$

and $\vec{\mathrm{p}}_m=p_m\hat{\eta}$. The scattered field $\vec{\mathrm{E}}_s(\omega)$ is then given by

$$\vec{\mathrm{E}}_s(\omega)=\frac{e^{ikr}}{r^2}(k^2)[\vec{\mathrm{p}}_t-\hat{r}(\hat{r}\cdot\vec{\mathrm{p}}_t)]\ , \tag{39}$$

where

$$\vec{p}_t = -9\alpha_t(\omega_0)\alpha_t(\omega)(\cos^2\zeta \sin\theta' \hat{\theta}' + \sin\zeta \cos\zeta \sin\theta' \hat{\phi}') .$$

$\alpha_t(\omega_0)$ and $\alpha_t(\omega)$ are given by

$$\alpha_t(\omega_0) = \frac{(\epsilon_1+2\epsilon_2)-(a/r')^3(\epsilon_1-\epsilon_2)}{(\epsilon_2+2)(\epsilon_1+2\epsilon_2)+2(a/c)^3(\epsilon_2-1)(\epsilon_1-\epsilon_2)} ,$$

$$\alpha_t(\omega) = \frac{\epsilon_2'[(\epsilon_1'+2\epsilon_2')-(a/r')^3(\epsilon_1'-\epsilon_2')]}{(\epsilon_2'+2)(\epsilon_1'+2\epsilon_2')+2(a/c)^3(\epsilon_2'-1)(\epsilon_1'-\epsilon_2')} . \tag{40}$$

We can now proceed as before to calculate the enhancements averaged over a layer of molecules at r', G_{layer}, and over the entire spherical shell, G_{shell}. These are the same as in Eqs. (36) and (37), respectively, except that $\alpha_r(\omega_0)$ and $\alpha_r(\omega)$ are replaced by $\alpha_t(\omega_0)$ and $\alpha_t(\omega)$.

IV. NUMERICAL RESULTS

The dielectric constants for silver and gold used in this section have been taken from Johnson and Christy.[33] The dielectric constant of the dye layer which simulates Rhodamine B was calculated from[20]

$$\epsilon_2 = 1 + s/(\omega_0^2 - \omega^2 - i\omega\tau) ,$$

where ω is the incident frequency, $\omega_0 = 3.5\times10^{15}$ sec^{-1}, $s = 5\times10^{30}$ sec^{-2}, and $\tau = 2.5\times10^{14}$ sec^{-1}. The external medium is taken to be air.

A. Extinction of dye-coated Ag, Au, and dielectric spheres

The coupling between the dye and the silver is illustrated in Fig. 2 by plots of extinction versus wavelength for 5-nm radius spheres with a/c varying from 0 (pure dye) to 1 (pure silver). Calculations in this section utilize the boundary-value solution based on the full series expansion[22] and so although the results in Fig. 2 might have been approximated with the electrostatic solution, it has been possible here to explore size effects such as will be shown in Fig. 3.

We note in Fig. 2, even for the pure dye particle, that the resonance peak 510 nm has shifted significantly from that for the bulk dye which is at 580 nm. Also the peak for the silver particle at 350 nm differs significantly from that near 400 nm in our earlier work[13] where the external medium was taken as water. Indeed, in water, for which the dielectric constant more closely approaches the dipolar surface-plasmon resonance condition ($\epsilon \rightarrow -2$), the extinction at the peak is much greater.

One effect of increasing coating thickness is a slight shift of the silver peak to lower wavelengths. Increasing size of the silver core has a greater impact on the dye peak which shifts from 510 to 450 nm as the radius of the silver core increases from 0 to 0.99 of the outer radius. It can also be seen that the dye peak reaches the maximum when the a/c ratio is about 0.6. This means proper combination of silver core and dye coating will produce a dye peak larger than that of a pure dye sphere. There

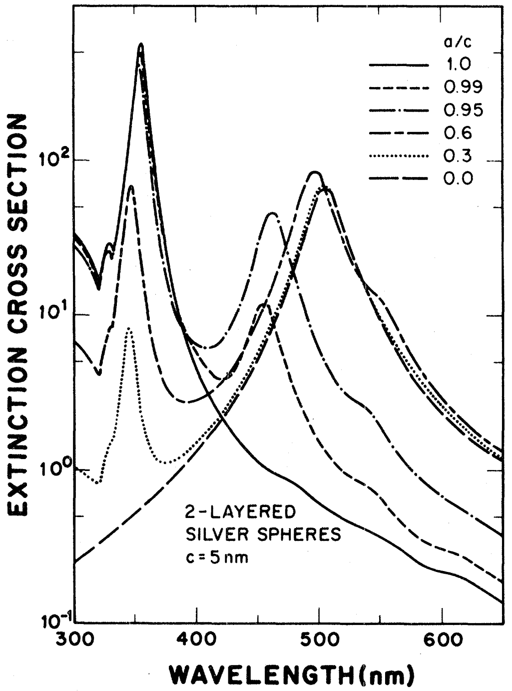

FIG. 2. Extinction cross section vs wavelength for silver spheres coated with concentric spherical shells of dye with various thicknesses. The ratio of core radius to total radius is a/c. The radius c is 5 nm.

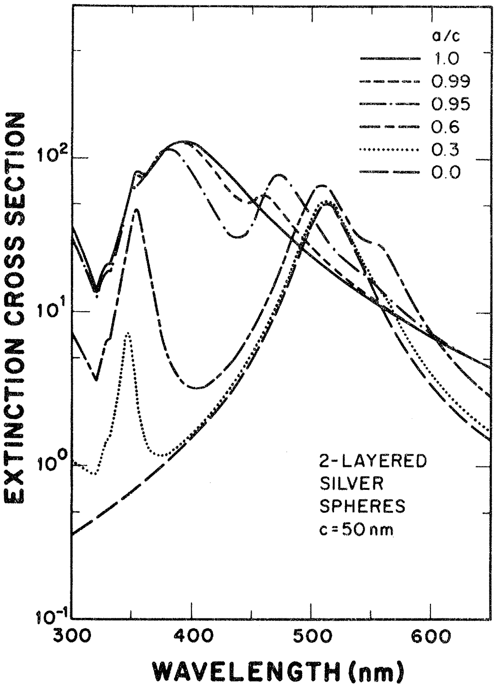

FIG. 3. Same as Fig. 2 for $c=50$ nm.

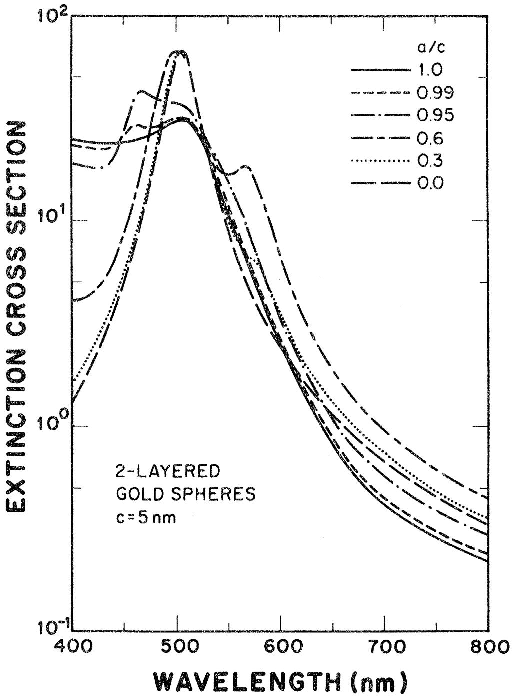

FIG. 4. Same as Fig. 2 for gold cores.

is also a slight enhancement of the extinction peak upon insertion of the small silver core. At about 425 nm, extinction of the pure dye and pure silver particles are equal and less than for any compound body at that wavelength. Accordingly, at 425 nm the extinction will be enhanced either by a coating of dye on the silver particle or by insertion of a small silver core into the dye particle.

Figure 3 provides an illustration of the effect of particle size. We have already noted that these calculations are sufficiently general to permit exploration of this aspect. The narrow extinction band of the small silver particle ($a=5$ nm), which is associated with the dipolar silver plasmon, is now very much broadened for this somewhat larger particle ($a=50$ nm) reflecting the contribution of higher multipoles to the extinction. It should be noted that this particular radius is still considerably smaller than the wavelength. The narrow silver band reappears as a/c decreases, corresponding to a successively smaller silver core. However, the magnitude of the silver peak is lower than that in Fig. 2 due to the thicker dye coating. Less electromagnetic radiation penetrates the dye coating to reach the silver core. The effect of increasing the size of the silver core on the extinction band of the dye is qualitatively similar to what has already been seen to occur in the case of the smaller particle. However, with this larger particle, contributions from additional multiples, both from the silver and the dye moieties, no longer permit the identification of particular resonant modes.

A quite different situation is apparent for a 5-nm dye-coated gold particle (see Fig. 4). The extinction peak for the gold and dye particles near 510 nm are very close. These peaks split in the coated spheres but because the initial bands are so broad, these are not well resolved. The extinction of the gold particle is considerably greater than that of the dye particle in the ultraviolet and the extinction varies monotonically as a/c changes from 0 to 1. At higher wavelengths, the extinction of the dye particle is greater and the variation of the extinction with a/c is no longer monotonic. Indeed the extinction when $a/c=0.6$ is greater than for either of the pure particles.

Figure 5 illustrates the interaction of a dye coating with a dielectric core which in this case is taken to have a constant refractive index ($m_1=1.5$, $\epsilon_1=2.25$). The dielectric sphere ($a/c=1$) shows the usual λ^{-4} dependence. The extinction band of the dye particle splits upon insertion of a dielectric core, i.e., whereas for a small homogeneous sphere there is a single resonant mode, for a small spherical shell there are two such modes. This can be seen from the limiting expressison for the polariza-

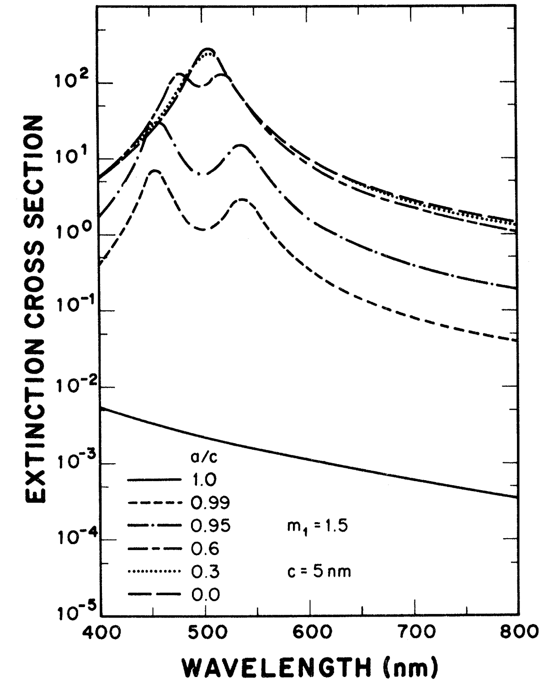

FIG. 5. Same as Fig. 2 for cores with refractive index $m_1 = 1.5$.

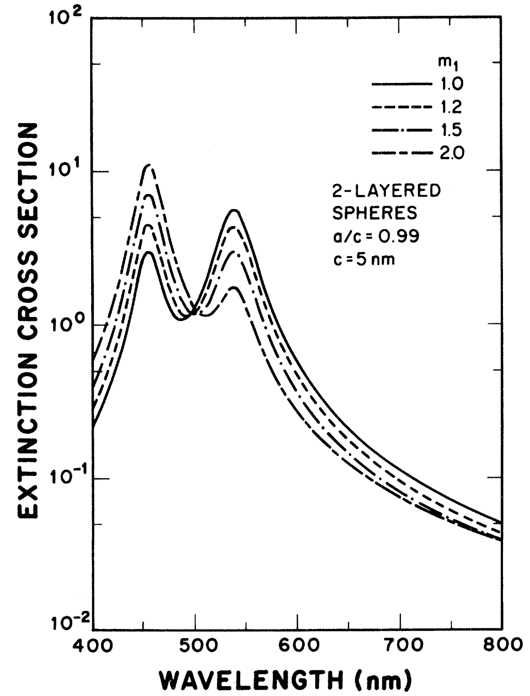

FIG. 6. Same as Fig. 2 for $a/c = 0.99$, and cores with various constant real refractive indexes.

bility of a small concentric sphere[21]:

$$\alpha=\frac{(\epsilon_1-\epsilon_2)(2\epsilon_2+1)(a/c)^3+(\epsilon_2-1)(2\epsilon_2+\epsilon_1)}{2(\epsilon_1-\epsilon_2)(\epsilon_2-1)(a/c)^3+(\epsilon_2+2)(2\epsilon_2+\epsilon_1)} . \tag{41}$$

Since the denominator of Eq. (41) is a second-order function of ϵ_2, α has two maxima for which there will be corresponding peaks in the extinction.

The effect of varying the refractive index of the dielectric core is shown in Fig. 6 for a fixed dye thickness, $a/c = 0.99$. Although the relative height of the peaks varies with refractive index of the core, the extent of the splitting is unaffected. Interestingly, but not surprisingly according to Eq. (41), the splitting is observed even for $m_1 = 1.0$. A system for possible observation of this effect would be lipid vesicles into which a fluorescent dye has been inserted.[34]

B. Extinction of dye-coated, randomly oriented Ag, Au, and dielectric spheroids

The very great sensitivity of SERS to particle shape[13] as a metal sphere coated with a monolayer is deformed to a spheroid, has been shown to be directly related to the corresponding dependence upon shape of the extinction cross section, *provided* the particle is sufficiently small (electrostatic case). Accordingly, we now explore the effect of shape upon the extinction of small particles coated with a layer of dyes both because of an intrinsic interest in extinction by such systems and because, for sufficiently small particles, there is most likely to be a direct correlation between extinction and both luminescence and SERS. We have not yet succeeded in applying our general model for luminescence and SERS to layered spheroids of any size.

The extinction cross section as a function of wavelength is depicted in Fig. 7 for two-layered silver prolate spheroids for which the coating is given by $q = l/a = 0.99$. The eccentricity of the spheroid varies from $a/b = 1$ to 3. The former case ($a/b = 1$), which corresponds to the appropriate curve in Fig. 2, displays the peaks associated with extinction by the silver and by the dye. For a spheroid these peaks should split in accordance with the two-fold degeneracy of the polarizability of a spheroid as illustrated by the separate expressions for the polarizabilities $\alpha_{\parallel}$ and $\alpha_{\perp}$ [Eq. (2) and Eq. (17)]. Although the splitting of the silver peak can be clearly seen in Fig. 7, there does not appear

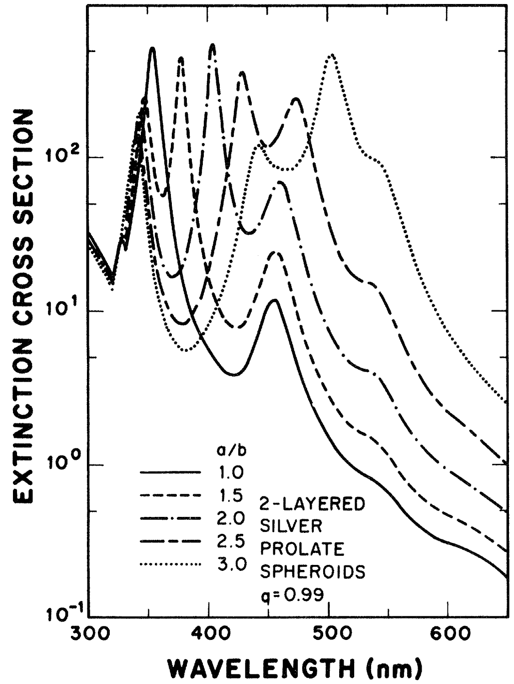

FIG. 7. Extinction cross section vs wavelength for silver spheroids coated with confocal spherical shells of dye. The ratio of inner to outer axis $l/a = q = 0.99$. The various eccentricities are given by a/b.

to be a corresponding effect for the dye. For $a/b = 1.5$ and 2.0, any splitting is obscured by the rather broad width of the dye extinction band. For more eccentric spheroids ($a/b = 2.5$, 3.0), there is a distinct shift to higher wavelength which indicates that the peak has split but that the dye peak at the lower wavelength has now interfered with the longer-wavelength silver peak which has now moved into this region. In any case the extinction spectrum of the more eccentric spheroid is quite different from that of the sphere so that a corresponding shift in the dependence of luminescence or SERS upon the excitation wavelength is to be expected.

Figure 8 for a somewhat thicker layer of dye ($q = 0.95$) displays the splitting to the extinction bands quite explicitly, particularly the example for which the eccentricity is $a/b = 2.5$. There are five distinct peaks: two at 330 and 430 nm derived from Ag, two at 510 and 610 nm derived from the dye, and another at 480 nm which could be due to the interaction between the silver core and the dye coating.

The sensitivity of the extinction cross section itself to the thickness of the coating is shown in Fig. 9 for $a/b = 2.5$ at 610 nm and for $a/b = 3.0$ at 503 nm. In this case the abscissa is $(a - l)/a$.

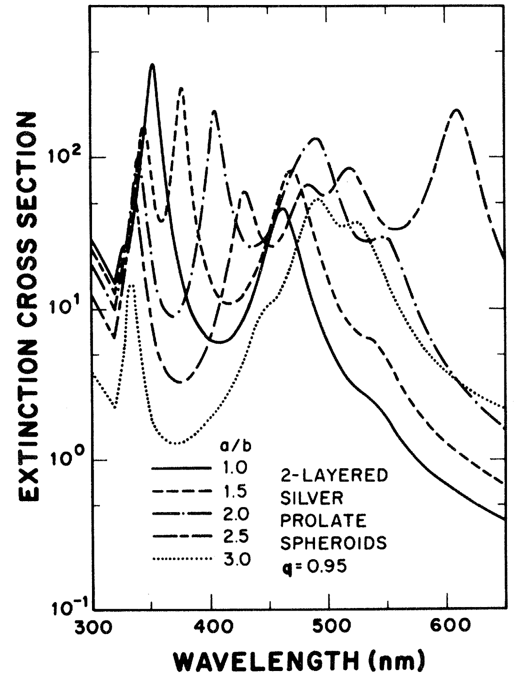

FIG. 8. Same as Fig. 7 for $q = 0.95$.

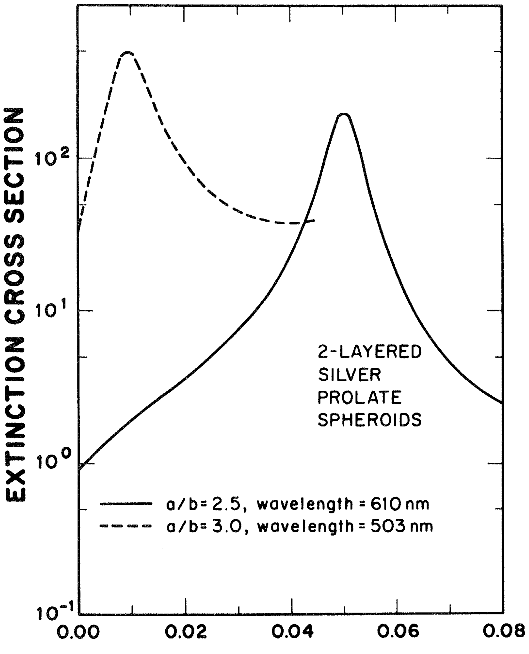

FIG. 9. Extinction cross section vs dye thickness $(a - l)/a$ [designated $(/a)$] for silver spheroids coated with confocal spherical shells of dye for $a/b = 2.5$, $\lambda = 610$ nm, and for $a/b = 3.0$, $\lambda = 503$ nm.

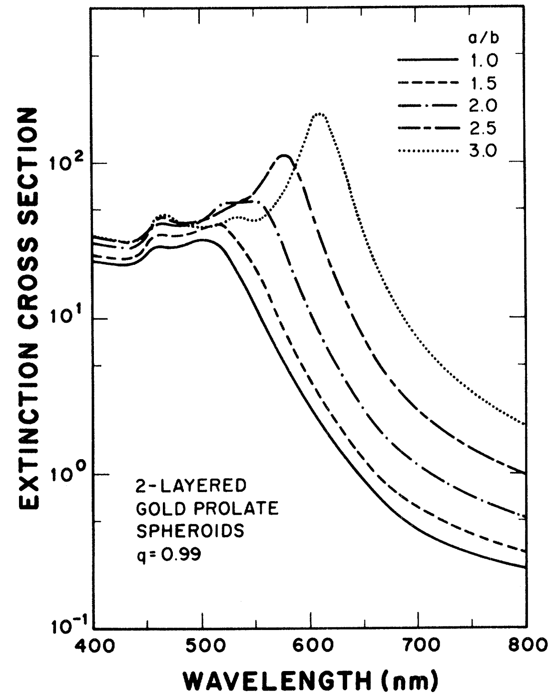

FIG. 10. Same as Fig. 7 for gold.

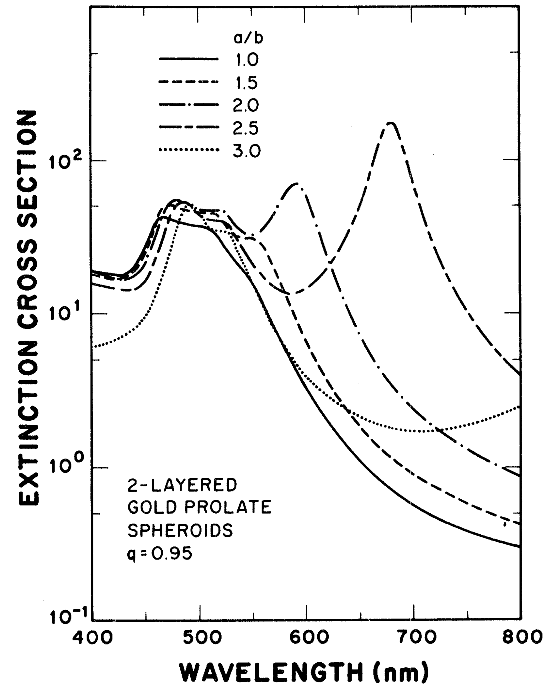

FIG. 11. Same as Fig. 8 for gold.

Two comments are in order in connection with the great sensitivity of the extinction to both shape (Fig. 8) and coating thickness (Fig. 9). The effects displayed here for dye-coated silver particles in air are even further enhanced when the particles are immersed in water since, as already noted, the dielectric constant of Ag relative to that of water more nearly approaches the value for excitation of the dipolar surface plasmon. Moreover, the great sensitivity of the extinction to morphology of both the silver and dye moities suggests that there will be similar effects for SERS and luminescence. Accordingly, it would not be surprising to observe large differences between signals measured from dispersions or surfaces which, although prepared in a similar manner, exhibit only slight morphological differences.

That each particular metal may respond differently is illustrated in Fig. 10 for gold cores with a dye coating of $q = 0.99$. We have already noted that the extinction cross section for a dye-coated gold sphere does not exhibit much structure because of the overlap of the corresponding extinction bands of the gold and dye particles. However an interesting feature here is the development of a sharp band at longer wavelengths as the particle becomes increasingly eccentric. This parallels the appearance of a dipolar surface plasmon in homogeneous gold spheroids which had been theoretically explored earlier[13] and which can lead to SERS enhancements for gold spheroids even greater than those for silver. Once again we note that the effects reported here for gold and silver in air are even further enhanced when the calculations are performed with water as the dispersion medium.

Figure 11 illustrates the effect for gold spheroids of increasing the dye thickness to $q = 0.95$. The shift of the gold dipolar surface plasmon to longer wavelength is even greater, indeed for $a/b = 3.0$ the peak in off scale at a wavelength somewhat in excess of 1000 nm. At 680 nm the extinction increases by nearly 10^3 as the sphere is extended to an equivolume spheriod with $a/b = 2.5$ and then decreases by 10^2 with further extension to $a/b = 3.0$.

There are no comparable effects when the core is a dielectric as shown in Fig. 12 for $m_1 = 1.5$ and $q = 0.99$. We have already seen that the extinction band for a small dye sphere is split when the dye comprises a spherical shell on a dielectric core and that the spectrum is not very sensitive to the dielectric constant of the core. Here we see also that there is very little effect of shape upon the spectrum as the concentric sphere is deformed to a

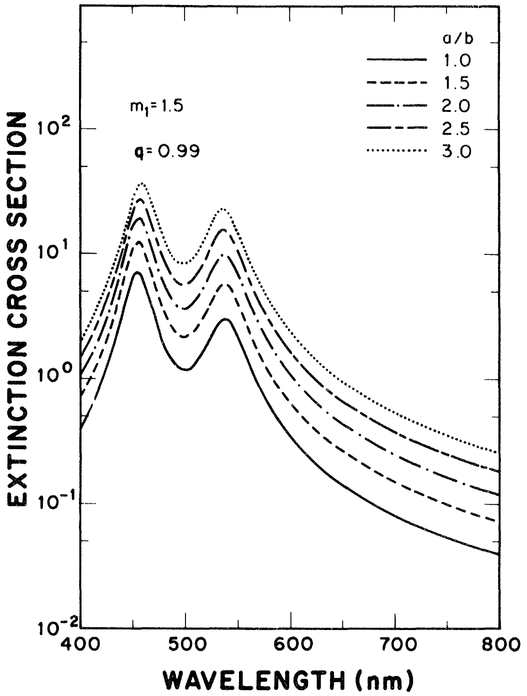

FIG. 12. Same as Fig. 7 for dielectric core, $m_1 = 1.5$.

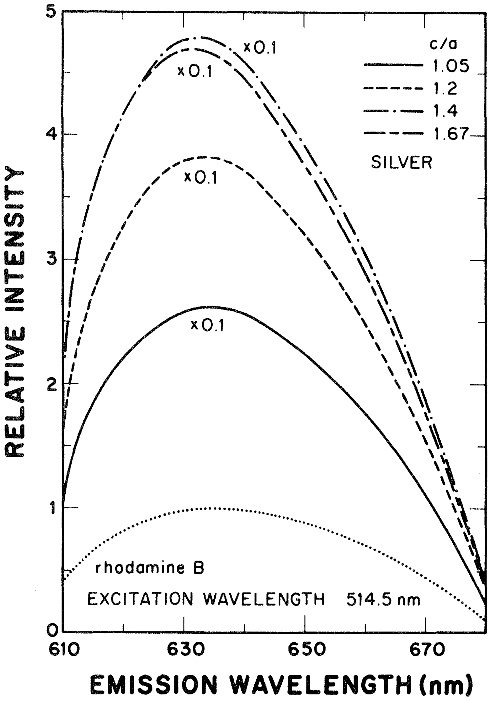

FIG. 13. Relative intensity of luminescence of dye-coated silver spheres (small-particle limit) at various wavelengths and coating thicknesses for excitation by $\lambda = 514.5$.

confocal spheriod. A similar result was obtained for the case of a somewhat thicker layer of dye, i.e., $q = 0.95$.

C. Enhancement of luminescence by dye-coated metal spheres

This work has been stimulated by reports of measured enhancement of luminescence by dye molecules adsorbed on metal island films[17] as well as our own plans to study comparable colloidal dispersions. The model differs from that for SERS in that the active molecules, taken as electric dipoles, are now embedded in a layer of finite thickness, coating the metal core, which has the bulk dielectric constant of the dye. In the SERS work[8,10,13] the active dipoles are presumed to vibrate in the external medium, viz., water or air. Otherwise, although we will refer here to luminescence, the model is equally applicable to either SERS or luminescence.

The external medium is taken here to be air in order to correspond to the already reported experimental work.[17] However, once again we stress that much larger calculated enhancements both of extinction and luminescence are obtained when the external medium is water, because then the optical constants of silver and gold more closely approach the dielectric constant corresponding to excitation of the dipolar surface plasmon.

The computations in this section are for the limiting case that the particle is small compared to the wavelength. Although the model has been formulated for concentric spheres of any size and optical constants,[30] that formulation is not utilized here because it requires considerable additional programming and computational time.

In Fig. 13 and emission spectra for various coating thicknesses (specified by c/a) are compared with that for pure rhodamine B.[35] The relative intensity is obtained by multiplying the emission of pure rhodamine B by the calculated enhancement at each shifted wavelength for excitation at 514.5 nm. The maximum in the emission shifts only slightly from 640 nm for pure rhodamine B to 630 nm for a particle with $c/a = 1.67$. The enhancement itself varies from 26 for $c/a = 1.05$ to about 48 for $c/a = 1.4$.

Note that in Fig. 13 the enhancement is lowered for $c/a = 1.67$. This effect of coating thickness is shown in Fig. 14 for Ag, Au, and Cu cores. The enhancements for these metals are of comparable magnitude at these excitation and emission wavelengths. In each case there is an intermediate layer

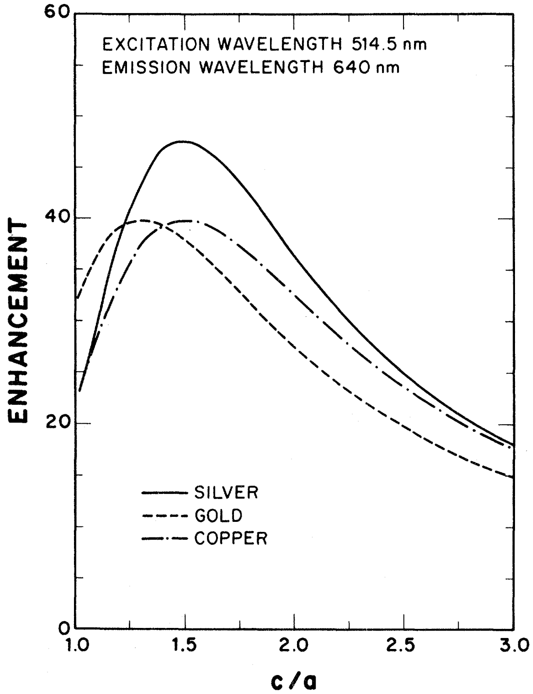

FIG. 14. Enhancement of luminescence of dye-coated silver, gold, and copper (small-particle limit), as a function of coating thickness.

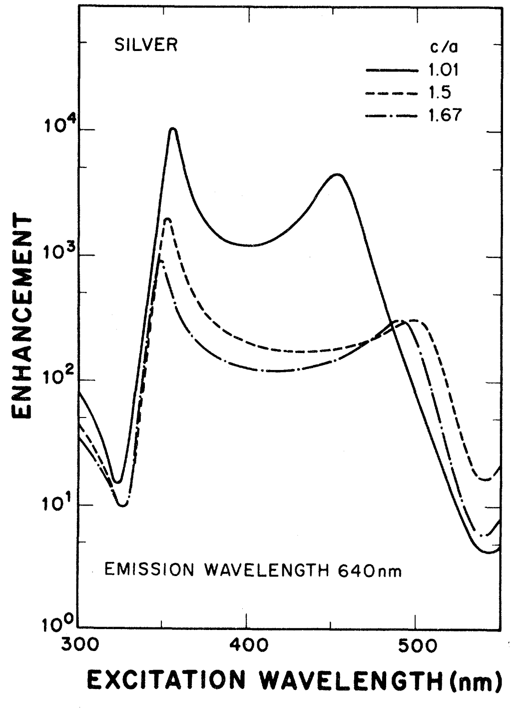

FIG. 15. Enhancement of luminescence of dye-coated silver spheres (small-particle limit) of various coating thicknesses vs excitation wavelength. Emission wavelength is 640 nm.

thickness which gives maximum enhancement. Since the enhancement is normalized to the number of active molecules, this means that molecules somewhat removed from the metal-dye interface make the greatest contribution to the enhancement. This is evident as we discussed earlier in connection with Figs. 2 and 9 in which a certain layer thickness gives a maximum extinction cross section at a fixed wavelength. The much smaller values of the enhancement here are due mainly to the use of air rather than water as the dispersion medium as well as to the fact that the excitation and emission wavelengths do not correspond to those for optimum excitation of the electromagnetic (EM) fields.

Figures 15 and 16 show the effect of excitation wavelength for Ag and Au particles with three thicknesses of dye layer. Emission is taken in the middle of the dye emission spectrum ($\lambda = 640$ nm). The broad double band for silver in the range to 350 to 450 nm corresponds to tuning the excitation into the corresponding extinction band shown in Fig. 2. Indeed the change of enhancement band with thickening dye layer reflects approximately the corresponding change in the extinction band. The corresponding effects for gold (Figs. 4 and 16) are somewhat more subtle, but still definitely indicated.

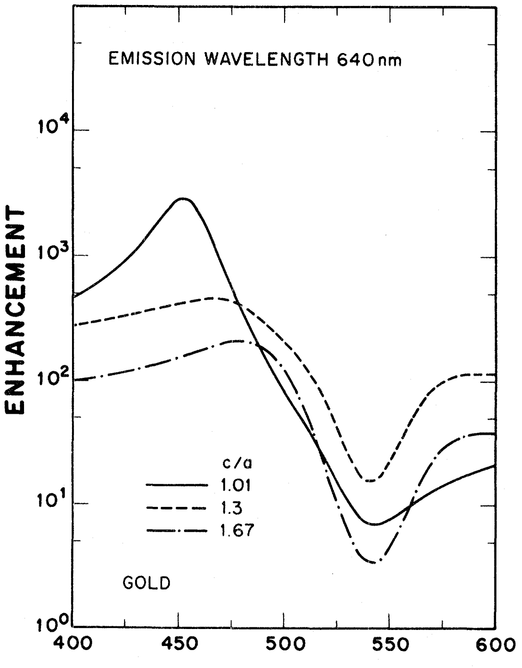

FIG. 16. Same as Fig. 15 for gold.

Figures 15 and 16 also indicate the substantial influence of coating thickness on enhancement. This influence may differ considerably at different excitation wavelengths, Thus, for both Ag and Au the enhancement drops sharply with coating thickness in the near ultraviolet. On the other hand, the opposite trend occurs at longer wavelengths.

V. SUMMARY

We note the following:

(1) The extinction cross section for a randomly oriented spheroid coated with a confocal spheroidal shell is given in the small-particle (electrostatic) limit by Eq. (17).

(2) The enhancement of luminescence of a sphere coated with a concentric spherical shell of luminescent material is given in the small-particle (electrostatic) limit by Eq. (34), for the case that the moments of the dipoles simulating the luminescent molecules are parallel to the radius vector. For dipoles oriented perpendicular to the radius vector the polarizabilities $\alpha_t(\omega_0)$ and $\alpha_t(\omega)$ given by Eq. (40) must be substituted into Eq. (34).

(3) For concentric spheres interaction between dye coating and core display a number of features:

(a) When the sharp extinction bands for the small pure particles are well separated such as for silver and dye, the peaks are shifted in the compound particle.

(b) For larger particles, the contributions from higher multipoles tend to wash out the distinct peak structure.

(c) Interaction between dye and metal extinction bands is much less pronounced when the metal and dye bands overlap as in the case of the dye-coated gold particles.

(d) The extinction band of a small dye particle is split whenever the dye comprises a coating on a dielectric core, even when the dye is merely a bubble, i.e., the core has a refractive index of unity.

(4) For confocal spheroids:

(a) Each of the extinction bands associated with the metal core and the dye coating split into two bands.

(b) There may be enhancement of the extinction which goes through a sharp maximum of 2 orders of magnitude as the thickness is increased.

(c) Whereas both the shift of the extinction band and its enhancement are much more sensitive to eccentricity for gold cores than for silver, the splitting of the dye extinction band on a dielectric core is insensitive to spheroid eccentricity.

(5) A number of features pertaining to the luminescence of dye coated metal spheres are:

(a) The shape of the emission spectrum is only moderately different from that of the pure dye.

(b) The enhancement of luminescence goes through a maximum as the dye thickness varies.

(c) The enhancement of luminescence is particularly sensitive to the excitation wavelength; indeed it parallels roughly the wavelength dependence of the extinction. Very large enhancements are obtained at those wavelengths when the extinction is large.

(d) Were the particles to be immersed in water rather than in air as in the present study, the enhancements of both luminescence and extinction would be greater.

ACKNOWLEDGMENTS

This work was supported by grants from the National Science Foundation (CHE-8011444) and the Army Research Office (DAAG-29-79-6-005).

---

[1] P. P. Van Duyne in *Chemical and Biological Applications of Lasers,* edited by C. B. Moore (Academic, New York, 1978), Vol. 4.

[2] T. H. Wood and M. V. Klein, Solid State Commun. 35, 263 (1980).

[3] J. G. Bergman, D. S. Chemla, P. F. Liao, A. M. Glass, R. H. Hart, and D. H. Olson, Opt. Lett. 6, 33 (1981).

[4] J. A. Creighton, C. G. Blatchford, and M. G. Albrecht, Trans. Faraday Soc. II 75, 790 (1979).

[5] M. Kerker, O. Siiman, L. A. Bumm, and D.-S. Wang, Appl. Opt. 19, 3253 (1980).

[6] K. V. Von Raben, R. K. Chang, and B. L. Laube, Chem. Phys. Lett. 79, 465 (1981).

[7] M. Moskovits, J. Chem. Phys. 69, 4159 (1978).

[8] D.-S. Wang, H. Chew, and M. Kerker, Appl. Opt. 19, 2256 (1980).

[9] S. McCall, P. M. Platzman, and P. A. Wolff, Phys. Lett. 77A, 381 (1980).

[10] M. Kerker, D.-S. Wang, and H. Chew, Appl. Opt. 19, 4159 (1980).

[11] J. Gersten and A. Nitzan, J. Chem. Phys. 73, 3023 (1980).

[12] F. J. Adrian, Chem. Phys. Lett. 78, 45 (1981).

[13] D. S. Wang and M. Kerker, Phys. Rev. B 24, 1777 (1981).

[14] M. Faraday, Philos. Trans. R. Soc. London 147, 145 (1857).

[15] G. Mie, Ann. Phys. 25, 377 (1908).

[16] J. C. Maxwell-Garnett, Philos. Trans. R. Soc. London 203, 385 (1904); 205, 237 (1906).

[17] A. M. Glass, P. F. Liao, J. G. Bergman, and D. H. Olson, Opt. Lett. 5, 368 (1980).

[18] J. E. Rowe, C. V. Shank, D. A. Zwemer, and C. A. Murray, Phys. Rev. Lett. 44, 1770 (1980); C. A. Murray, D. L. Allara, and M. Rhinewine, *ibid.* 46, 51 (1981); T. H. Woul, D. A. Zwemer, C. V. Shank, and J. E. Rowe, Chem. Phys. Lett. 82, 5 (1981).

[19] S. Garoff, D. A. Weitz, T. J. Gramila, and C. D. Hanson, Opt. Lett. 6, 245 (1981).

[20] H. G. Craighead and A. M. Glass, Opt. Lett. 6, 248 (1981)

[21] A. Guttler, Ann. Phys. (Leipzig) 11, 65 (1952).

[22] A. L. Aden and M. Kerker, J. Appl. Phys. 22, 1242 (1951).

[23] R. R. Bilboul, J. Phys. D 2, 921 (1969).

[24] M. Kerker, J. Opt. Soc. Am. 65, 376, 1085 (1975).

[25] C. F. Eagen, Appl. Opt. 20, 3035 (1981).

[26] H. Chew P. J. McNulty, and M. Kerker, Phys. Rev. A 13, 396 (1976).

[27] M. Kerker, P. J. McNulty, M. Sculley, H. Chew and D. D. Cooke, J. Opt. Soc. Am. 68, 1676 (1978).

[28] H. Chew, M. Sculley, M. Kerker, P. J. McNulty, and D. D. Cooke, J. Opt. Soc. Am. 68, 1686 (1978).

[29] M. Kerker and S. Druger, Appl. Opt. 18, 1172 (1979).

[30] H. Chew, M. Kerker, and P. J. McNulty, J. Opt. Soc. Am. 66, 440 (1976).

[31] H. Chew, D. D. Cooke, and M. Kerker, Appl. Opt. 19, 44 (1980).

[32] D.-S. Wang, M. Kerker, and H. Chew, Appl. Opt. 19, 2315 (1980).

[33] P. B. Johnson and R. W. Christy, Phys. Rev. B 6, 4370 (1972).

[34] N. Duzgunes, J. Wilschut, R. Fraley, and D. Papahadjopoulous, Biochim. Biophys. Acta. 642, 182 (1981).

[35] *Handbook of Fluorescence Spectra of Aromatic Molecules,* edited by I. Berlman (Academic, New York, 1971).